The structural, chemical, and electronic properties of a stable GaS/GaAs interface

X. A. Cao,[a] H. T. Hu, Y. Dong, X. M. Ding, and X. Y. Hou
Surface Physics Laboratory, Fudan University, Shanghai 200433, People's Republic of China

(Received 14 May 1999; accepted for publication 7 September 1999)

A stable GaS passivating layer was deposited on GaAs using α-Ga_2S_3 powder as a single-source precursor. Both good crystal quality and clean GaS/GaAs interface were achieved. Electron-energy-loss spectra showed that the sulfide material has a band gap of 3.0 eV. The valence band discontinuity of the heterostructure was determined to be 1.9 eV from a series of ultraviolet photoelectron spectra with increasing deposition thickness. Al/GaS/GaAs metal-insulator-semiconductor structures exhibited typical high frequency capacitor versus voltage ($C-V$) behavior with very small loop hysteresis. The $C-V$ curves showed no aging after 20 months. © *1999 American Institute of Physics.* [S0021-8979(99)00424-7]

I. INTRODUCTION

The passivation of III–V compound semiconductors, especially GaAs, remains an unsolved problem in device technology. In 1987, Sandroff[1] proposed that treatment of GaAs by using Na_2S solution rinsing could improve the material surface quality significantly. Since then, sulfur passivation has attracted considerable attention.[2–14] It has proven to be an efficient technique to enhance the photoluminescence response and benefit the performance of GaAs-based minority-carrier devices. Jeong *et al.*[6] deposited P_3N_5 as a gate dielectric on $(NH_4)_2S$ treated GaAs surface. The resultant metal-insulator-semiconductor field effect transistor (MISFET) showed good linearity and low hysteresis in current–voltage ($I-V$) characteristics. Small drain current drift was achieved due to the high quality P_3N_5/GaAs interface. The superior passivating effects of the sulfurizing treatments are often attributed to the formation of Ga–S bonds, terminating the GaAs surface,[2–5] which dramatically reduces surface recombination velocities, and to some extent, removes the Fermi level pinning.

Convenient and efficient passivation can be achieved by immersing the GaAs sample in sulfur-containing solutions such as $(NH_4)_2S$, or exposing it to sulfur-containing gases such as H_2S. However, these conventional treatments generally result in only one monolayer of sulfur atoms bonded to the GaAs surface,[2] which is electronically effective, but chemically unstable. The main cause of the subsequent degradation of the properties is reoxidization of the passivated surface.

It has demonstrated that a thick robust sulfide layer can improve the passivation durability significantly.[9] MacInnes[10] reported the chemical vapor deposition of a metastable face-centered-cubic phase of GaS on GaAs. MISFETs based on this structure showed good transconductance and input-to-output isolation.[11] In addition, the hexagonal phase of GaS can also be used to realize good passivation for GaAs. Hou *et al.*[12] reported an increase by two orders of magnitude in the photoluminescence yield of GaAs after a ''native'' hexagonal β-GaS formation. The breakdown strength of this dielectric was measured to be $>1\times10^6$ V/cm.[13]

In this article, we report an alternative passivation technique to grow stable hexagonal GaS on the GaAs (100) surfaces by vaporizing α-Ga_2S_3. X-ray diffraction (XRD), in conjunction with other techniques, was employed to examine the crystal quality. X-ray photoelectron spectroscopy (XPS) was used to study the chemical composition near the passivation film/substrate interface. The energy band structure was investigated by a combination of ultraviolet photoelectron spectroscopy (UPS) and electron-energy-loss spectroscopy (EELS). Finally, the electronic properties of the GaS/GaAs interface were evaluated by $C-V$ measurements.

II. EXPERIMENT

Single-crystal wafers of *n*-type, Te-doped GaAs(100), with a doping concentration $\sim10^{17}\,cm^{-3}$, were used in the experiments. The substrate was first cleaned in an ultrasonic bath with acetone, ethanol, and deionized (DI) water in sequence for 5 min each and dried by a jet of filtered N_2, then dipped in S_2Cl_2:$CCl_4=1:2$ solution to remove the native oxide and form a S-terminated surface.[14] After another quick rinse (5 s) in CCl_4, acetone, ethanol, and DI water, the sample was loaded into an extended molecular beam epitaxy chamber on a VG ADES-400 angle-resolved electron spectrometer with a base pressure of 10^{-7} Pa. Prior to growth, the substrate was heated to 500 °C for 20 min to remove the residual sulfur and other contaminants. The sulfide film was deposited by evaporating polycrystalline α-Ga_2S_3 powder from a Knudsen cell source. The substrate was maintained at 200 °C. Growth rates were monitored by a quartz microbalance at room temperature. Mass spectrometry was used to examine the vaporization composition as a function of

[a]Present address: Department of Materials Science and Engineering, University of Florida, Gainesville, Florida 32611; electronic mail: xcao@mail.mse.ufl.edu

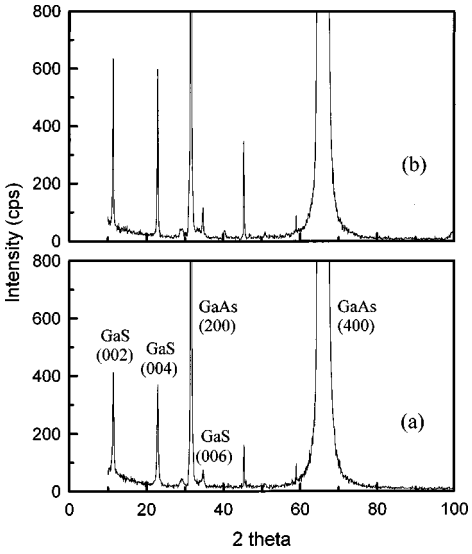

FIG. 1. XRD spectra for a 80-nm-thick GaS deposited on GaAs(100), (a) as-grown, (b) annealed at 500 °C for 6 min.

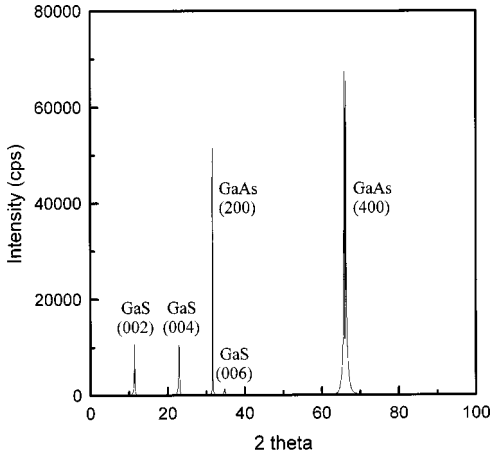

FIG. 2. XRD pattern of the GaS(400 nm) on GaAs(100).

source temperature. It was confirmed that Ga_2S_3 decomposed at ~720 °C in a vacuum condition through the reaction:

$$2Ga_2S_3(s) \rightarrow 4GaS(s) + S_2(g).$$

The stoichiometric GaS is vaporized at this temperature and crystallizes on the GaAs surface.

Several *ex situ* or *in situ* analysis techniques were employed to characterize the passivated samples. The sulfide composition and contamination were checked by Auger electron spectroscopy (AES). The material structure was examined by XRD with x-ray sources of Cu $K_{\alpha 1}$ ($\lambda = 0.154\,06$ nm) and $K_{\alpha 2}$ ($\lambda = 0.154\,44$ nm) lines. In addition, the crystalline quality was further examined by Raman spectroscopy. Depolarized spectra were recorded in the $X(YY)X$ scattering configurations at room temperature. *In situ* XPS, UPS, and EELS measurements were carried out in the main chamber of the ADES system with base pressure in the 10^{-8} Pa range. The x-ray source was Al $K\alpha$ line with a photon energy of 1486.6 eV. The UV light source used was He I with a photon energy of 21.2 eV. The energy of the incident electron in EELS was 30 eV.

Finally, Al/GaS/GaAs MIS diodes were fabricated by evaporating AuGe/Ni/Ti/Au on the backside of the GaAs substrate as the ohmic contact and 1-mm-diameter aluminum dots on an 80-nm-thick GaS as the gate electrodes. The substrate in this case was a 2-μm-thick molecular beam epitaxy *n*-type GaAs(100) layer with doping concentration of $5 \times 10^{16}\,cm^{-3}$ on a heavily Si-doped GaAs wafer. High frequency (1 MHz) $C-V$ measurements were conducted with a 50 mV/s sweep rate at room temperature.

III. RESULTS AND DISCUSSION

The growth of GaS on GaAs initiated with several monolayers of amorphous structure due to the large lattice mismatch. However this material has a strong tendency to crystallize, and different peaks from various planes of hexagonal β-GaS crystal could be clearly recorded by an ordinary x-ray diffractometer after a 40 nm deposition. Two prominent peaks corresponding to the GaS(002) and GaS(004) are evident in Fig. 1(a), when the thickness increased to 80 nm. The lattice constants are $a = b = 0.3587$ nm, and $c = 1.5492$ nm. β-GaS has a layered structure, with four sheets of hexagonal close-packed atoms in such a manner that the Ga–Ga bonds are sandwiched by sheets of sulfur atoms.[15] The XRD results indicate that growth along the *c* axis (i.e., perpendicular to the substrate surface) is favorable. Figure 1(b) shows the diffraction from the same sample after annealing at 500 °C for 6 min. The crystalline quality was improved since the intensities of the GaS peaks increased by a factor of ~2. It is worth noting that a disordered layer at the interface would not degrade the passivating effectiveness. This is in analogy with the fact that amorphous SiO_2 can protect Si both electronically and chemically.

Figure 2 shows XRD scans from 400 nm thick GaS on GaAs(100). The doublets appearing in the spectrum are due to nonmonochromatic x-ray sources (i.e., coexistence of both Cu $K_{\alpha 1}$ and $K_{\alpha 2}$ lines). Since the two dominating peaks are from two planes parallel with each other, the film grown is nearly single crystal.

Auger surface scans revealed the O KLL signal is well below the detection limit in the bulk of the overlayer and at the GaS/GaAs interface. This oxygen-free growth is critical

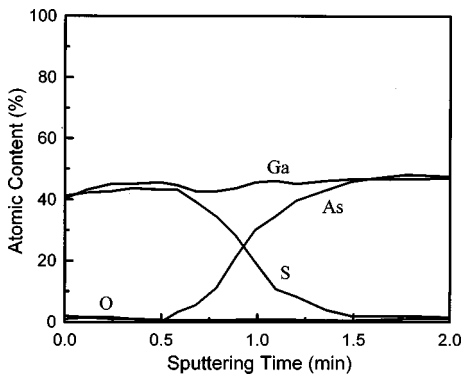

FIG. 3. AES depth profile of the GaS passivated GaAs sample.

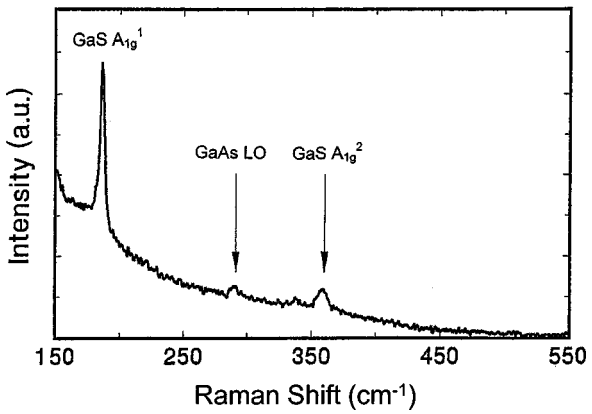

FIG. 4. Depolarized Raman spectrum for the GaS(400 nm) on GaAs.

to achieve long-term reliable passivation. We determined the compositions from peak-to-peak heights of the Ga, As, S, and O signals, and the relative atomic sensitivity factors, which have been verified by Rutherford backscattering measurements. The obtained AES depth profile is shown in Fig. 3. As expected, the atomic ratio of Ga to S is close to 1:1 in the film. The sputtering rate of the Ar^+ ion gun is ~10 nm/min, and thus the width of the transition region can be estimated to be ~5 nm. The interface appears quite abrupt by taking into account profile broadening due to sputtering effects and the inelastic mean free path of the photoelectrons.

The crystal quality was further examined by Raman scattering. Figure 4 shows the depolarized Raman spectrum excited from a film of 400 nm. It clearly reveals A_{1g}^1 and A_{1g}^2 phonon modes of the hexagonal GaS lattice at 188 and 360 cm^{-1}, respectively. These modes involve motion of the Ga ions relative to each other[16] and are typical active modes in β-GaS, which has D_{6h}^4 symmetry. The feature at 291 cm^{-1} in the spectrum corresponds to the LO phonon line in the GaAs substrate.

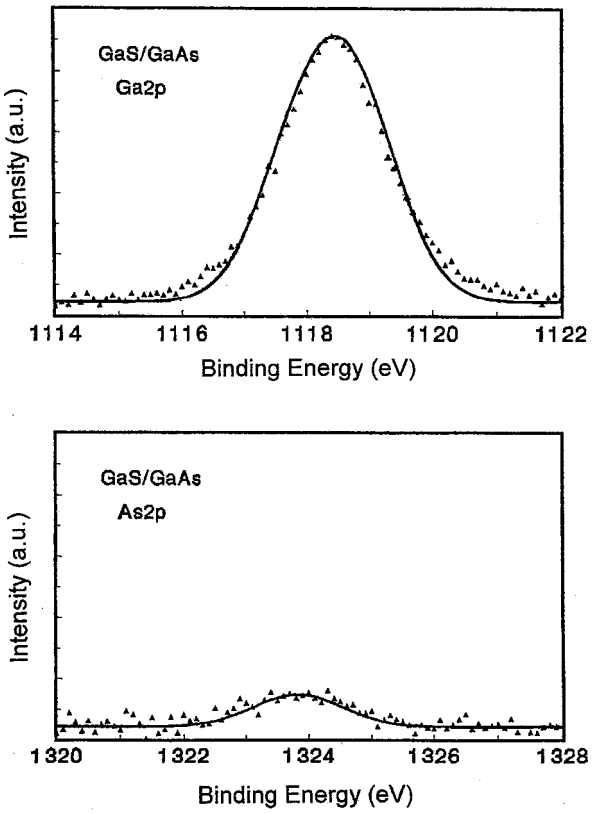

FIG. 5. The As $2p$ (bottom) and Ga $2p$ (top) XPS spectra of the GaS passivated GaAs(100) surface.

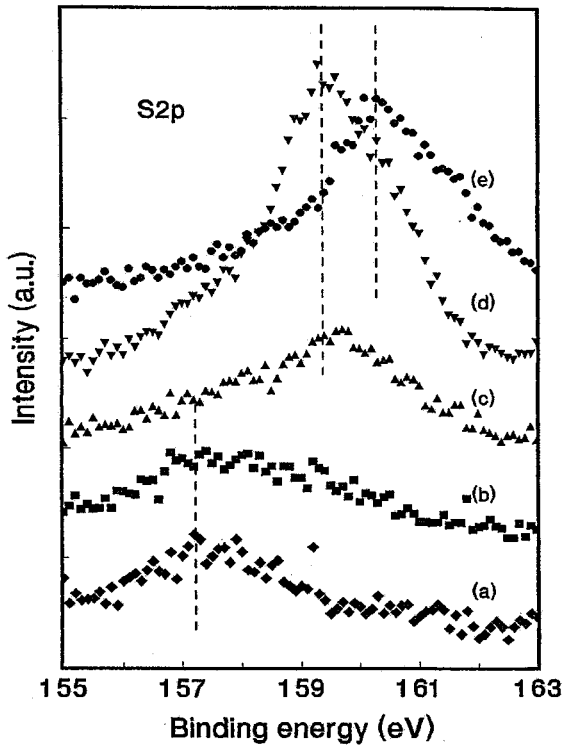

FIG. 6. The S $2p$ core-level spectra for (a) bare GaAs surface, (b) GaS (0.1 nm/GaAs, (c) GaS (1.5 nm)/GaAs, (d) GaS (7 nm)/GaAs, and (e) sample d annealed at 500 °C for 20 min.

Figure 5 shows the As $2p$ and Ga $2p$ core-level spectra after several monolayers of deposition. The Ga $2p$ data can be fitted by two components with different binding energies. The peak with lower binding energy originates from the Ga atoms bonded with As in the substrate. Meanwhile, the peak with a chemical shift of ~1.0 eV can be attributed to the Ga atoms bonded with sulfur atoms. In the case of the As $2p$ spectrum, only the signal from the substrate is observed. This demonstrates no As outdiffusion occurred at the GaS/GaAs interface during the growth.

Figure 6 shows S $2p$ spectra for the bare GaAs substrate (a), 0.1 nm GaS on GaAs (b), 1.5 nm GaS on GaAs (c), 7 nm GaS on GaAs (d), and sample (d) after annealing at 500 °C for 20 min (e). The spectrum (a) is actually the contribution from the Ga $3s$ core level. As the thickness of GaS increased, the S $2p$ signal with the main peak at the binding energy of ~160 eV became more intense. After annealing, the component at the lower binding energy decreased, probably due to loss of the elemental S. Some S was incorporated into the GaS unintentionally during the deposition.

In situ EELS measurements were conducted for the as-grown GaS and samples annealed at 500 °C for 20 min. The spectra in Fig. 7 show the same threshold energy of 3.0 eV

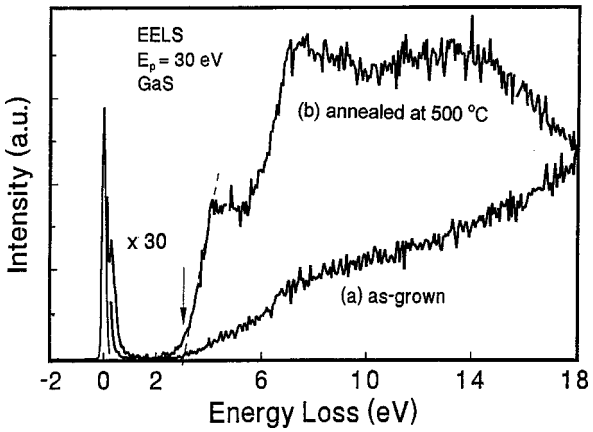

FIG. 7. EELS for the GaS passivating layer on GaAs(100), (a) as-grown, (b) annealed at 500 °C for 20 min.

which corresponds to a strong direct interband transition at Γ point.[17] Note that the electron-energy-loss structure changed after annealing. However, the EELS resolution is not high enough to reveal the detailed distribution of valence electron states in this case. This was further studied by UPS measurements, as described below.

To get a complete picture of band lineup of the GaS/GaAs heterostructure, we need to determine the band discontinuities. Figure 8 shows a series of UPS spectra for the GaS on GaAs with increasing thickness. The top and bottom spectra present the energy distribution of the valence band for the GaS overlayer and GaAs substrate, respectively. The valence-band edges for these two materials are both evident

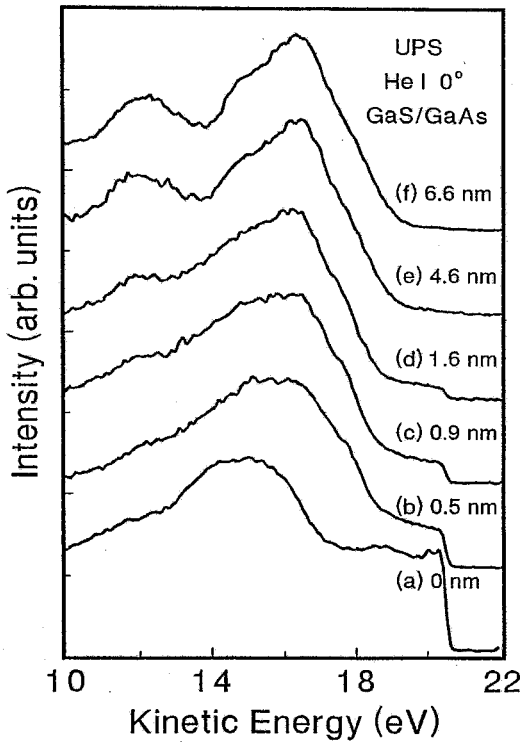

FIG. 8. UPS spectra for the GaS overlayers with increasing thickness on GaAs(100).

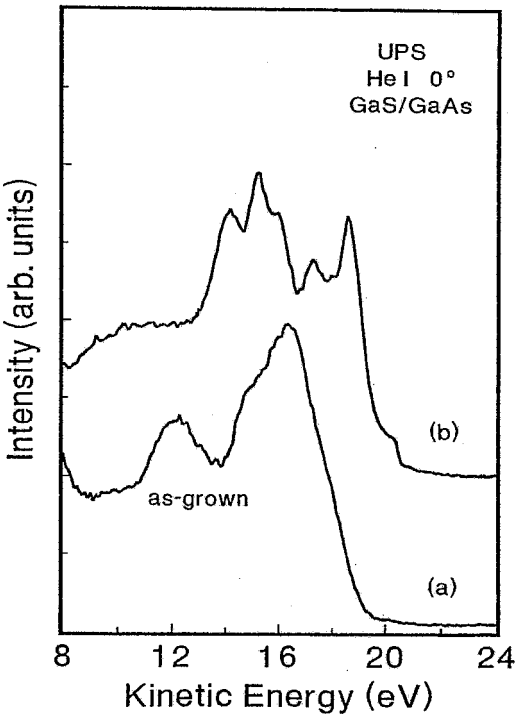

FIG. 9. UPS spectra for the GaS overlayers on GaAs(100), (a) as-grown, (b) annealed at 500 °C for 20 min.

in curve (b), (c), and (d), and the band offset can be determined to be 1.9 eV. Note that the energy difference in the valence-band maximum in curve (a) and (f) is 1.5 eV. It suggests a band bending of 0.4 eV at the interface, which mainly occurs at the GaS side, as can be seen in Fig. 8. Combined with the result from EELS, the conduction band discontinuity can be derived to be 0.3 eV. It is clear that the grown GaS has a weak *n*-type background, possibly due to the S-rich deposition as demonstrated by XPS data.

Figure 9 compares the He I spectrum for as-deposited

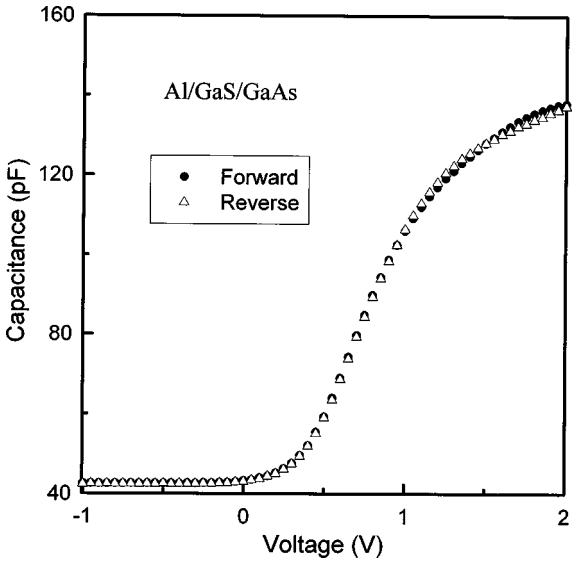

FIG. 10. High frequency (1 MHz) $C-V$ curves of the GaS/GaAs MIS diode at room temperature.

GaS and samples annealed at 500 °C for 20 min. In the latter case, considerable structures can be observed within the region $E_{vb}-10$ eV. These principle features are believed to derive from the *p*- and/or *s*-like valence electrons of Ga and S.[17] As also shown in Fig. 9, the S $3p$ peak located at a binding energy of about 10 eV is reduced by the annealing. Again, we ascribe this to removal of the elemental S. We cannot yet explain the new states showing up near the valence band maximum after annealing. The UPS results showed the improvement of the crystalline quality after thermal treatment. This agrees quite well with XRD and EELS measurements.

$C-V$ measurements were carried out to evaluate the electronic properties of the passivated GaAs surface. The MIS $C-V$ curves at room temperature measured at the frequency of 1 MHz is shown in Fig. 10. It can be seen that the clockwise loop hysteresis, which is a typical feature of GaAs MIS structures, is eliminated. Furthermore, the MIS diode characteristics were not subject to aging, even after 20 months. The breakdown strength of this passivation material was found to be $>1.5\times10^6$ V/cm after annealing. These results confirmed a stable and well-passivated GaS/GaAs interface, which is promising for the realization of new material gated GaAs MISFETs.

IV. CONCLUSION

We have demonstrated that β-GaS grown on GaAs(100) by using simple vapor deposition has near single crystalline structure with oxygen contamination below Auger detection limits. Detailed conduction-band structure and energy band lineup of the GaS/GaAs heterostructure have been revealed by a combination of UPS and EELS. MIS $C-V$ curves showed no observable loop hysteresis. This new passivating technique involves a common precursor and a simple facility, and is quite compatible with the existing GaAs technology. The extended characterization of the GaS layer and its feasibility as the gate dielectric in potential GaAs MIS structures will be the subject of a future report.

[1] C. J. Sandroff, R. N. Nottenberg, J. C. Bischott, and R. Bhat, Appl. Phys. Lett. **51**, 33 (1987).
[2] C. J. Spindt, D. Liu, K. Miyano, P. L. Meissner, T. T. Chiang, T. Kendelewiez, I. Lindau, and W. E. Spicer, Appl. Phys. Lett. **55**, 861 (1989).
[3] Z. H. Lu and M. J. Graham, Phys. Rev. B **48**, 4604 (1993).
[4] H. Hirayama and Y. Matsumoto, Appl. Phys. Lett. **54**, 2565 (1989).
[5] T. Ohno and K. Shiraishi, Phys. Rev. B **42**, 11194 (1990).
[6] Y. H. Jeong, K. H. Choi, S. K. Jo, and B. Kang, Jpn. J. Appl. Phys., Part 1 **34**, 1176 (1995).
[7] W. S. Hobson, F. Ren, U. Mohideen, R. E. Slusher, M. L. Schnoes, and S. J. Pearton, J. Vac. Sci. Technol. A **13**, 642 (1995).
[8] X. A. Cao, X. Y. Hou, X. Y. Chen, R. S. Zhou, Z. S. Li, X. M. Ding, and X. Wang, Appl. Phys. Lett. **70**, 747 (1997).
[9] X. Y. Hou, W. Z. Cai, Z. Q. He, P. H. Hao, Z. S. Li, X. M. Ding, and X. Wang, Appl. Phys. Lett. **60**, 2252 (1992).
[10] A. N. MacInnes, M. B. Power, and A. R. Barron, Appl. Phys. Lett. **62**, 713 (1993).
[11] P. P. Jenkins, A. N. MacInnes, M. Tabib-Azar, and A. R. Barron, Science **263**, 1751 (1994).
[12] X. Y. Hou, X. Y. Chen, Z. S. Li, X. M. Ding, and X. Wang, Appl. Phys. Lett. **69**, 1429 (1996).
[13] X. Y. Chen, X. Y. Hou, X. A. Cao, X. M. Ding, L. Y. Chen, G. Q. Zhao, and X. Wang, J. Cryst. Growth **173**, 51 (1997).
[14] Z. S. Li, W. Z. Cai, R. Z. Su, G. S. Dong, X. M. Ding, X. Y. Hou, and X. Wang, Appl. Phys. Lett. **64**, 3425 (1994).
[15] H. Hahn and G. Frank, Z. Anorg. Allg. Chem. **278**, 340 (1955).
[16] J. P. Van der Ziel, A. E. Meixner, and H. M. Kasper, Solid State Commun. **12**, 1213 (1973).
[17] E. Doni, R. Gilanda, V. Grasso, A. Balzarotti, and M. Piacentini, Nuovo Cimento **51**, 154 (1979).